Journal of Thermal Analysis and Calorimetry, Vol. 93 (2008) 3, 937–945

β-CRYSTALLISATION TENDENCY AND STRUCTURE OF POLYPROPYLENE GRAFTED BY MALEIC ANHYDRIDE AND ITS BLENDS WITH ISOTACTIC POLYPROPYLENE

A. Menyhárd[1,2*], *G. Faludi*[1] *and J. Varga*[1]

[1]Laboratory of Plastics and Rubber Technology, Department of Physical Chemistry and Materials Science at Budapest University of Technology and Economics, 1111 Budapest, Műegyetem rkp. 3. H. ép. I., Hungary
[2]Institute of Materials and Environmental Chemistry, Chemical Research Center at Hungarian Academy of Sciences, 1025 Budapest, Pusztaszeri út 59–67, Hungary

Crystallization, melting and structure of three different commercial types of isotactic polypropylene (iPP) grafted by maleic anhydride (PP-g-MAH) with different maleic anhydride content (AC) and their β-nucleated versions were studied by X-ray diffractometry (WAXS), differential scanning calorimetry (DSC), polarised light microscopy (PLM) and scanning electron microscopy (SEM). The presence of maleic anhydride units disturbs the chain regularity, hereby decreases the crystallization tendency of iPP in general and the β-crystallisation ability in particular. β-modification of iPP (β-iPP) forms only in β-nucleated PP-g-MAH polymers studied if the anhydride content is not larger than 0.5 mass%. The influence of AC of PP-g-MAH on the feature the spherulitic structure is demonstrated by PLM and SEM micrographs. The β-nucleated iPP/PP-g-MAH blends containing 10 mass% PP-g-MAH crystallise predominantly in β-form independently of AC of the latter. The β-nucleated blends of iPP and PP-g-MAH with lowest AC crystallise in β-form in whole concentration range. The interaction parameter between iPP and PP-g-MAH polymers calculated by Nishi–Wang equation indicate limited interaction between the components.

Keywords: *DSC, interaction parameter, iPP blends, iPP grafted by maleic anhydride, β-nucleation, supermolecular structure*

Introduction

Isotactic polypropylene (iPP) is one of the most commodity polymers used in the largest quantity today. Its good mechanical properties and relatively low price result in continuous growth of its production and expansion of its market. Its continuously increasing application accelerates research on all related fields, including the preparation of iPP based composites and blends. The preparation of polymer blends is an important technique in order to modify the target property of an individual polymer according to the requirement of the application field. iPP based blends are widely studied and discussed in the literature. The review paper of Utracki and Duomulin [1] summarises the most important experimental observations related to iPP based blends.

iPP is a crystalline polymer with three different polymorphic modifications, which are the monoclinic α-, the trigonal β- and the orthorhombic γ-form [2]. The β-modification of iPP (β-iPP) has some advantageous properties compared to that of the traditional α-form [3, 4] For example, its impact resistance is excellent [3–7]. Hence, there are several papers dealing with the preparation and investigation of the structure and properties of β-iPP and with the β-nucleated iPP blends [3, 4, 8–14] and composites [3, 4, 9, 15–17].

The iPP blends are usually heterogeneous systems [1]. In order to enhance the interaction between additive polymers and the iPP matrix on the interface compatibilizing agent are applied in practice. iPP grafted by maleic anhydride (PP-g-MAH) polymers are often used as compatibilizer in iPP/polyamide 6 (PA6) blends and in iPP based blends containing polar additive polymers [18–26]. The application of the compatibilizers lead to the formation of fine dispersion of the additive polymer in the matrix and to the improvement of the mechanical properties of the blends. The compatibilizer is expected to interact with both components of the blends. The anhydride group of the compatibilizer expected to form chemical bonds with PA6 and its iPP chain segments interact with the iPP matrix [20, 21]. In a recent work [26], we studied the crystallization, melting and structure of the iPP/PA6 blends compatibilized with PP-g-MAH polymers and their β-nucleated versions. It was found that the crucial condition for preparing iPP/PA6 blends containing a β-iPP matrix is the prevention of selective incorporation of the β-nucleating agent into the PA6 phase. It was demonstrated clearly that the

* Author for correspondence: amenyhard@mail.bme.hu

1388–6150/$20.00

Akadémiai Kiadó, Budapest, Hungary
Springer, Dordrecht, The Netherlands

Table 1 The characteristic properties of the PP-g-MAH polymers

Abbreviation	Properties
PP-g-MAH-I	POLYBOND 3150 (Uniroyal Chemical, USA) MFR=50 g (10 min)$^{-1}$ at 230°C and 2.16 kg AC=0.5 mass%, ρ=0.91 g cm^{-3}
PP-g-MAH-II	EXXELOR PO 1015 (Exxon, USA) MFR=150 g (10 min)$^{-1}$ at 230°C and 2.16 kg AC=1 mass%, ρ=0.9 g cm^{-3}
PP-g-MAH-III	LICOMONT AR 503 (Clariant, Switzerland) η=500–800 mPas at 170°C, AC=3 mass%, ρ=0.91 g cm^{-3}

distribution of the nucleating agent between the two phases could be influenced by the introduction of a compatibilizing agent.

One of the subjects of this work is to characterise the β-crystallisation tendency and the structure of some PP-g-MAH polymers used often as compatibilizer in iPP based blends. Several papers deal with the crystallisation and structure of PP-g-MAH and its blends with iPP [27–31]. The crystallisation tendency and morphology of these polymers differ from that of iPP, because of the presence of grafted anhydride units in polymer chain disturbing the chain regularity. Accordingly, Seo *et al*. [28] found that half crystallisation time is much smaller for PP-g-MAH than that for iPP. Bogoeva-Gaceva *et al*. [29] have observed with optical microscopy that the heterogeneous nucleation predominated in the case of PP-g-MAH, which resulted in spherulitic structure of lower average sizes. Similar conclusion was made from the analysis of crystallisation kinetics [28]. In the iPP/PP-g-MAH blends, co-crystallisation or phase separation of components may occur depending on the anhydride content (AC) of PP-g-MAH and on the thermal conditions of the crystallisation [21, 30, 31]. Duvall *et al*. [21] observed the formation of several spherulites of high birefringence in the iPP/PP-g-MAH blends. They assumed that these spherulites consist of the co-crystals. Subsequently, Varga and Ehrenstein [32] pointed out that these formations with high birefringence are β-spherulites induced by extended surface of the vacuum bubble appeared within the melt inclusion in the late stage of the crystallisation.

The β-crystallisation ability of PP-g-MAH polymers was studied in order to reveal the possibility of the application of PP-g-MAH as compatibilizer in β-nucleated iPP systems. Moreover, this work is dedicated to reveal the importance of the interaction between the compatibilizer and iPP matrix from the point of view of compatibilizing efficiency.

Experimental

Materials and methods

The Tipplen H-890 grade iPP homopolymer (MFR= 0.35 g/10 min at 230°C/2.16 kg, M_w=455300 g mol^{-1}, polydispersity of 3.7) supplied by Tisza Chemical Works (TVK, Hungary) was used as iPP component. Three types of PP-g-MAH were applied. Their characteristics are given in Table 1. It should be pointed out that the PP-g-MAH polymers studied differ not only in their anhydride content, but they have different molecular mass, molecular mass distribution. Moreover PP-g-MAH polymers are inhomogeneous on the level of chemical structure. They are mixture of polymers with different anhydride content. The β-nucleating agent was the Ca-salt of suberic acid, which was synthesised in our laboratory. The synthesis and β-nucleating efficiency and selectivity of this β-nucleating agent was described elsewhere [33].

The β-nucleated PP-g-MAH polymers and iPP/PP-g-MAH blends were homogenised at 200°C for 5 min and 50 rpm using a Brabender W 50 EH internal mixer. iPP/PP-g-MAH blends were prepared in the whole concentration range (0–100 mass% of maleated PP content). The melting and crystallization characteristics of the samples were studied by DSC using a Perkin Elmer DSC-7 apparatus, where the mass of the samples was between 3–5 mg. The heating and cooling rate was 10°C min^{-1} during all DSC scans. The temperature was calibrated by indium and zinc as reference materials. The thermal and mechanical prehistory of the samples was erased at 220°C for 5 min. In order to eliminate the disturbing effect of the βα-recrystallization during the determination of the polymorphic composition, the β-nucleated samples were cooled to the critical recooling temperature, T_R^*=100°C, during studying of non-isothermal crystallisation characteristics [8, 33]. The β-content (β_c) was determined from the partial area of the melting curve of β-phase recorded after this limited recooling step according to the following equation (Eq. (1)).

$$\beta_c = \frac{X_\beta}{X_\beta + X_\alpha} \quad (1)$$

where the β_c is the β-content, X_β and X_α are the degree of crystallinity of the α- and β-form respectively, which can be calculated by using the value of equilibrium enthalpy of fusion of the β- (113 Jg^{-1}) and α-iPP (148 Jg^{-1}) [3].

The supermolecular structure of the samples was studied by PLM and SEM techniques. PLM investigations

were carried out on a Leitz Dialux 20 optical microscope equipped by Polaroid DMC Model 1 digital camera and Image Pro Plus software. In order to determine the optical character of the samples studied, a λ-plate located diagonally between the crossed polarisers was used. Different temperature programs were applied during PLM studies using a Mettler FP82HT hot stage. The samples were crystallised under isothermal conditions after the elimination of thermal and mechanical prehistory. The samples were cooled to various crystallization temperatures (T_c) at a rate of 5°C min^{-1}, or quenched (uncontrolled cooling to T_c as fast as possible) and the structure formed during these isothermal experiments was registered by PLM.

SEM micrographs were taken from selected samples using a LEO 1540 XB equipment with a low energy electron beam at 1 kV. The samples were prepared on Mettler FP82HT hot stage. The thermal and mechanical prehistory was erased by heat treatment at 220°C for 5 min. Then the samples were quenched to the crystallisation temperature T_c=135°C and held there until they completely crystallised. The samples were etched with a permanganic solution according to the method introduced by Olley [34]. The etching was not successful in the case of PP-g-MAH-III, because it dissolves in the etching solution.

Wide angle X-ray scattering (WAXS) patterns were recorded using a Philips PW 1830/PW type equipment with CuK$_\alpha$ radiation at 40 kV and 35 mA. The scanning rate was 2° min^{-1}.

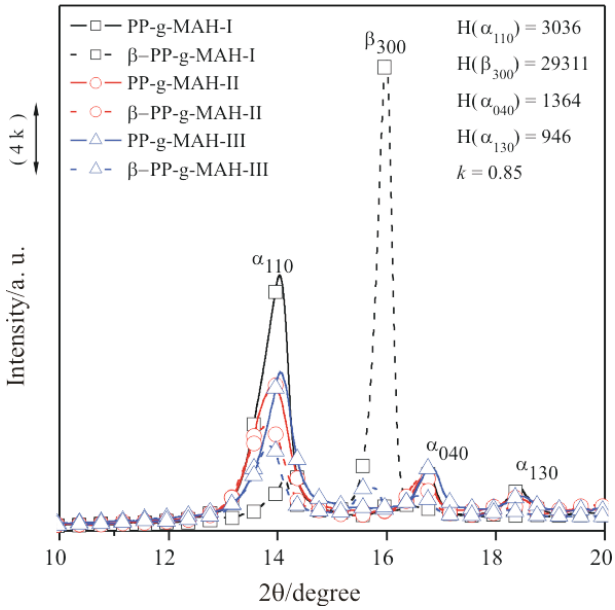

Fig. 1 WAXS patterns of the β-nucleated and non-nucleated PP-g-MAH polymers crystallised at T_c=120°C

Results and discussion

Structure, crystallization and melting characteristics of PP-g-MAH polymers

WAXS patterns of the non-nucleated and β-nucleated PP-g-MAH polymers are shown in Fig. 1. The non-nucleated samples crystallise in α-form as revealed by diffraction peaks of α_{110}, α_{040} and α_{130} at 2θ of 14.1, 16.8 and 18° respectively. Since the characteristic diffraction peak of β_{300} at 2θ of 16° comes into view only in this case β-nucleated PP-g-MAH-I with the lowest AC, it can stated that β-phase can form only in PP-g-MAH with low AC. The k value, which was introduced by Turner–Jones *et al*. [35] for the quanti-

Table 2 Crystallization and melting characteristics of non-nucleated and b-nucleated PP-g-MAH polymers recorded after cooling to T_R^*

Polymer type	Melting			Crystallization		
	$T_{mp}(\alpha)$/°C	$T_{mp}(\beta)$/°C	ΔH_m/J g^{-1}	T_{cp}/°C	ΔH_c/J g^{-1}	ΔT_c/°C
PP-g-MAH-I	162.7 168.4	–	93.5	110.1	–96.6	8.1
PP-g-MAH-II	141.8 150.1	–	69.4	98.0	–76.4	8.8
PP-g-MAH-III	141.5 152.4	–	50.1	101.3	–58.5	16.2
β-PP-g-MAH-I	167.4	152.9	93.9	124.3	–88.5	6.3
β-PP-g-MAH-II	141.7 149.7	–	59.0	101.0	–69.5	6.2
β-PP-g-MAH-III	140.0 150.7	–	50.1	104.8	–58.5	7.2

$T_{mp}(\alpha)$ – peak temperature of melting of the α-form, $T_{mp}(\beta)$ – peak temperature of melting of the β-form, ΔH_m – overall enthalpy of fusion recorded after limited recooling, T_{cp} – peak temperature of crystallization, ΔH_c – overall enthalpy of crystallization, ΔT_c – temperature range of crystallization ($\Delta T_c = T_{onset} - T_{end}$)

tative characterisation of the β-content, is about 0.85 for PP-g-MAH-I. This k-value is lower than that of iPP homopolymer, which is normally in the range of 0.9–1.0 in the samples nucleated by Ca-suberate [36]. Consequently, the β-crystallisation ability of PP-g-MAH polymers with increasing AC decreases and disappears at AC above of 0.5 mass%. The intensity of the diffraction peaks decreases with increasing AC indicating the reduced overall crystallinity.

The crystallisation curves of the non-nucleated and β-nucleated PP-g-MAH polymers (not showed) registered at cooling rate of 10°C min^{-1} have a single peak. The peak temperature (T_{cp}), temperature interval of the crystallisation (ΔT_c) and the enthalpy of crystallization (ΔH_c) were determined from the crystallisation curves. These characteristics are included in the Table 2. One can state that the higher the anhydride content of a PP-g-MAH is, the lower is its crystallization tendency. With increasing AC, T_{cp} shift towards to the lower temperature range, ΔH_c decreases and ΔT_c is widened. The crystallization peak of PP-g-MAH-III is the broadest (large ΔT_c value) since it contains the highest number of anhydride units along the chain. Moreover, it has lower molecular mass and higher polydispersity. It is worth to mention that the temperature interval of crystallization of all β-nucleated PP-g-MAH polymers is narrower than that of the non-nucleated samples. It means that the crystallization rate depends rather on the presence of nucleating agent, than on AC.

The melting curves of different PP-g-MAH samples are showed in Fig. 2. Based on melting curves, the melting peaks temperatures of α and β-modification ($T_{mp}(\alpha)$ and $T_{mp}(\beta)$) and the overall enthalpy of fusion (ΔH_m) were determined. They are collected in Table 2. With increasing AC, the enthalpy of fusion of PP-g-MAH polymers decreases and the melting peaks of non-nucleated are shifted to the lower temperature. The melting curve of nucleated of PP-g-MAH-I is located in lower temperature range than that of its non-nucleated version indicating the formation of β-form, which is in accordance with WAXS results. The presence of nucleating agent does not influence the melting characteristics of PP-g-MAH-II and III at all, their non-nucleated and nucleated versions melt in similar temperature range and the melting profiles are identical. In spite of that the melting of PP-g-MAH-II and PP-g-MAH-III occurs in similar temperature range as the melting of β-form, no β-modification is present in these samples according to the results of WAXS experiments. The melting curves have some special feature compared to that of pure iPP. In every case a double melting peak was registered. This peak multiplication can be explained by the perfection of the crystalline structure during heating superimposed on the endothermic melting process [37]. This indicates that an unstable structure is formed during the crystallization because of the lower crystallization tendency and higher undercooling ability.

PLM micrographs of iPP-g-MAH-I are shown in Fig. 3. The non-nucleated PP-g-MAH-I crystallises in α-modification forming well-developed negative α-spherulites in early stage of crystallisation (Fig. 3a). The formation of β-quasispherulites with strong negative birefringence and ovalites can be observed in the β-nucleated samples shown in Fig. 3b. These morphological units form from 'rod-like' precursors, which are hexagonites standing edge on, as it has been discussed in our earlier work in details [33, 38].

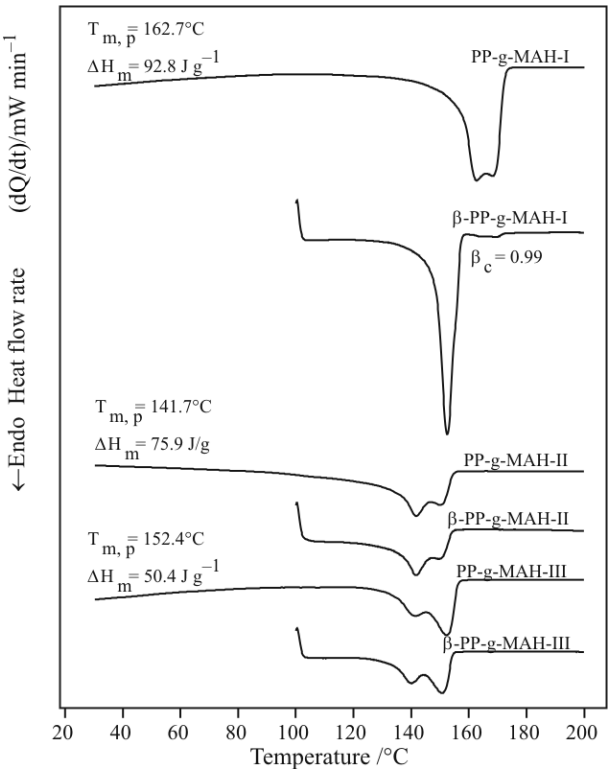

Fig. 2 The melting curves of non-nucleated PP-g-MAH polymers recorded during heating from room temperature (T_R=25°C) and that of their β-nucleated forms recorded after limited recooling (T_R^*=100°C)

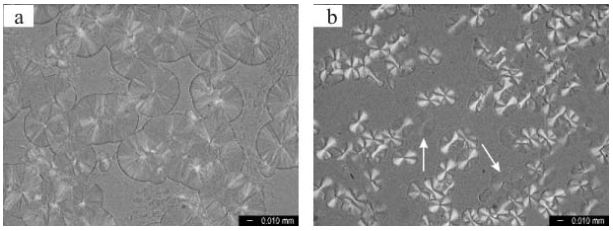

Fig. 3 PLM micrographs of the a – non nucleated PP-g-MAH I (T_c=130°C; t_c=10 min) and b – β-nucleated PP-g-MAH I (T=135°C; t=10 min)

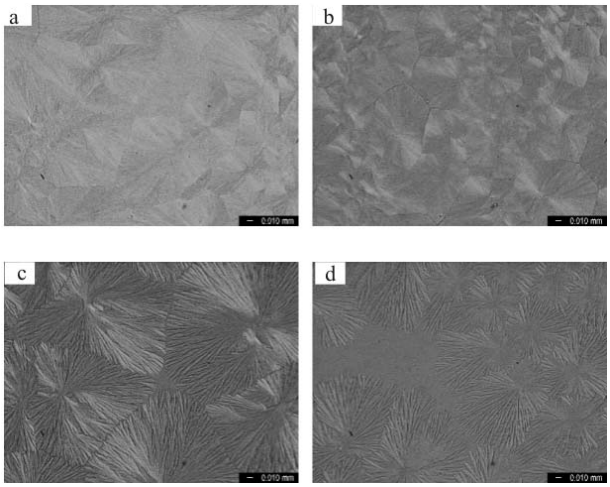

Fig. 4 PLM micrographs of the a – non nucleated PP-g-MAH II (T_c=130°C; t_c=45 min), b – β-nucleated PP-g-MAH II (T_c=135°C; t_c=45 min), c – non-nucleated PP-g-MAH III (T_c=130°C; t_c=10 min) and d – β-nucleated PP-g-MAH III (T_c=135°C; t_c=10 min)

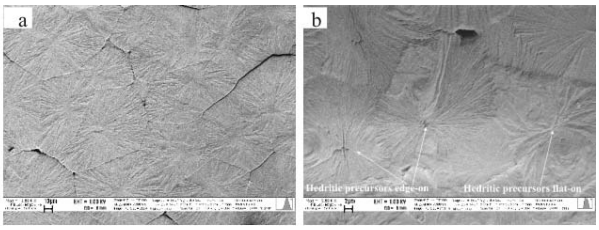

Fig. 5 Spherulitic structure of a – non-nucleated PP-g-MAH-I at 1000x and b – β-nucleated PP-g-MAH-I at 5000× magnification

A few α-spherulites form sporadically with low negative birefringence. (Showed by arrows). It should be noticed that the density of nuclei is higher in the presence of β-nucleating agent. In order to obtain better-developed β-spherulites, the PLM experiments with nucleated sample were carried out at higher temperature (135°C) (Fig. 3b).

The spherulitic structure of the other two types of PP-g-MAH is rather coarse and open and their birefringence is very low. One can observe the individual lamellae and lamellar branching even in the optical level. These two types of PP-g-MAH polymer are crystallised into α-form despite of the presence of highly active β-nucleating agent (Fig. 4). The lamellar structure of non-nucleated and β-nucleated PP-g-MAH-I is visualised by SEM micrographs in Fig. 5. The non-nucleated sample consists of α-spherulites with radial arrangement of lamellae (Fig. 5a). The lamellar arrangement in β-nucleated sample is similar to that of β-iPP and the quasispherulites have 'face-like' appearance (showed by arrows). These

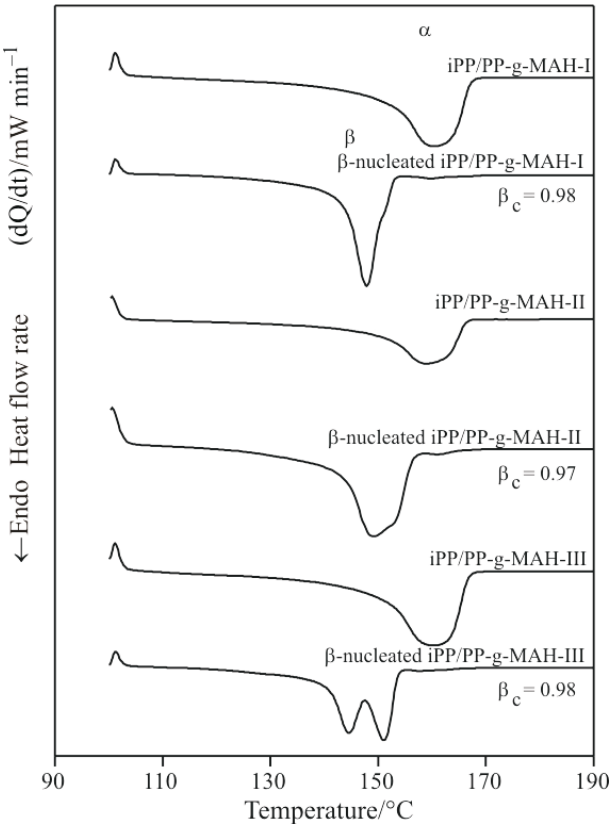

Fig. 6 Melting curves of iPP/PP-g-MAH blends and their β-nucleated versions recorded after limited recooling (T_R=100°C; PP-g-MAH content is 10 mass%)

were induced by hexagonite precursors standing edge-on [3, 33, 38]. Therefore, most of β-lamellae are seen edge-on as well. Nevertheless, a few flat-on β-lamellae are perceptible in the micrograph (Fig. 5b, showed by arrow).

Crystallization and melting and supermolecular structure of iPP/PP-g-MAH blends

The results mentioned above prove, that the high AC of PP-g-MAH polymers hinders the formation of β-modification. Therefore, it is worth to study the effect of PP-g-MAH on the crystallization process of β-nucleated iPP. These compatibilizers are used usually in small amount (1–5 mass%) in iPP blends. The concentration of the compatibilizers was selected a little above this value (10 mass%) in our experiments.

The DSC traces of the non-nucleated and β-nucleated blends iPP/PP-g-MAH containing 10 mass% of different PP-g-MAH polymers recorded after the limited recooling step are presented in Fig. 6. The double melting peaks located at about 150°C relate to the β-modification of iPP. All β-nucleated blends crystallise into β-form in the presence of the of PP-g-MAH types independently

on their AC value. It is worth to mention that the duplication of β-melting peaks becomes more pronounced with increasing AC of the compatibilizers. The melting peak multiplication can be related to the perfection process within the β-form and indicates increasing the structural instability of the β-form with increasing AC of compatibilizers. The results of our present and previous work [26] have revealed that all PP-g-MAH-s studied can apply in β-nucleated iPP based blends up to 10 mass% as compatibilizers.

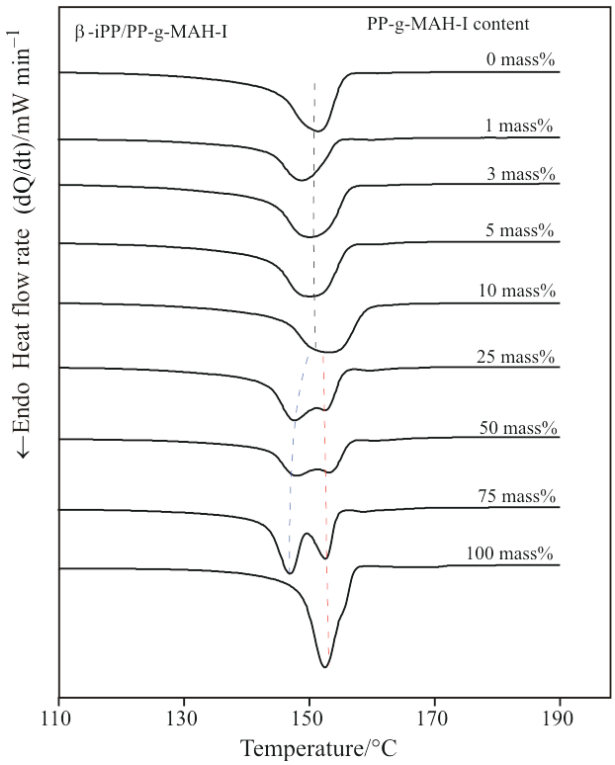

Fig. 7 The melting traces of β-nucleated iPP/PP-g-MAH-I blends recorded after limited recooling (T_R=100°C)

The β-nucleated iPP based blends containing PP-g-MAH-I additive polymer crystallise in the β-form in the whole concentration range. The melting curves registered after limited recooling (T_R=100°C) are plotted in Fig. 7. Similarly to the non-nucleated blends the double melting peaks of PP-g-MAH-I becomes more and more pronounced with its increasing content.

Interaction in iPP/ PP-g-MAH blends

According to the concept of mechanism of the compatibilization, the PP-g-MAH polymers might interact with iPP. In order to characterise the interaction between iPP and PP-g-MAH polymers, blends were prepared in the entire concentration range. The melting traces of non-nucleated iPP/PP-g-MAH blends are plotted in Fig. 8. The melting of PP-g-MAH-I with the smallest AC takes place in similar temperature range as iPP (Fig. 8a). The characteristic double melting peak of PP-g-MAH-I appears with increasing PP-g-MAH-I content above 10 mass% and it becomes more pronounced with further increase of compatibilizer content (Fig. 8a).

The melting traces of iPP/PP-g-MAH-II and III blends are more complicated than that of the previous ones, because the melting peak is shifted to the lower temperatures above 10 mass% of additive polymer content. The melting curves of iPP/PP-g-MAH-II blends are shown in Fig. 8b. At higher PP-g-MAH-II content

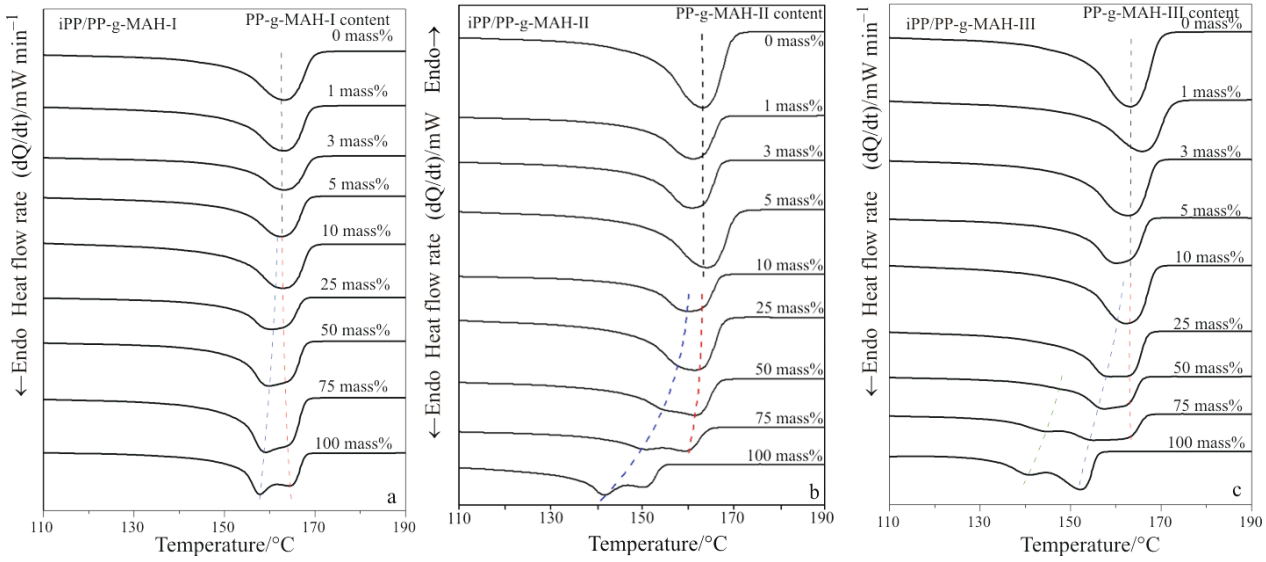

Fig. 8 Melting traces of non-nucleated iPP/PP-g-MAH polymer blends in whole concentration range recorded after limited recooling (T_R^*=100°C); a – iPP/PP-g-MAH-I, b – iPP/PP-g-MAH-II, c – iPP/PP-g-MAH-III

(above 10 mass%), the melting peaks break up and two different crystalline populations seems to be form indicating the possible phase separation. One of the crystalline populations can be related to that phase, which consists predominantly of iPP and melts at higher temperature (Fig. 8b). The other population appearing at lower temperature relates to that phase, which contains predominantly PP-g-MAH-II (Fig. 8b). Moreover, a steep depression of the peak temperature of melting can be observed with increasing of PP-g-MAH-II content.

In the case of PP-g-MAH-III, which has the largest anhydride content and low molecular mass, the components melt mostly separately. The double melting peaks of PP-g-MAH-III is detectable above 10 mass% similarly to the other two types and the intensity of its double melting peak increasing continuously with increasing of PP-g-MAH-III content (Fig. 8c). A slight depression of peak temperature of the double peak relating to the PP-g-MAH-III component is observable on the melting traces. Moreover, the intensities of the melting peak of iPP at highest temperatures and the double peak of PP-g-MAH-III at lower temperatures relate more or less proportionally to the composition of the blend. The melting peak of iPP component is at around 165°C independently of the content of PP-g-MAH-III. The melting peaks of PP-g-MAH-III shift to the lower temperature ranges with increasing of the PP-g-MAH-III content. These results suggest that there might be a weak interaction in the case of the presence of PP-g-MAH-I and III and a stronger interaction in the presence of PP-g-MAH-II.

According to the Flory–Huggins theory, the depression of the melting temperature relates to the interaction parameter (χ_{12}) through the following equation described by Nishi and Wang [39]:

$$\frac{1}{T_m}-\frac{1}{T_m^0}=\frac{RV_2}{\Delta H_2}\chi_{12}(1-\varphi_2)^2 \qquad (2)$$

where, T_m is the peak temperature of melting relating to the PP-g-MAH phase and T_m^0 is the equilibrium melting temperature of iPP, which is 208°C according to Monasse and Haudin [40]. χ_{12} is the polymer-polymer interaction parameter and φ_2 and $\varphi_1=1-\varphi_2$ are the volume fraction of iPP and PP-g-MAH polymers respectively. During the calculation of the volume fraction of PP-g-MAH polymers (φ_1) the crystallinity of iPP has been taken into account. The value of equilibrium enthalpy of fusion of iPP (148 J g^{-1} [41]) was determined by Monasse and Haudin and the density of the amorphous and crystalline part is 0.852 and 0.936 g cm^{-3} respectively. The V is the molar volume of repeating unit, which is not known in the case of PP-g-MAH, so we used the value of iPP (53.9 cm^3 mol^{-1} [42]) for both components. Due to these simplifications the calculations can result in only approximate results. ΔH_2 is the enthalpy of fusion of iPP (8778 J mol^{-1} [42]). Plotting the experimental results of $(1/T_m-1/T_m^0)$ *vs.* φ_1^2 ($\varphi_1=1-\varphi_2$) according to Equation 2 should result in a straight line and the value of χ_{12} consequently can be calculated from the slope. An example is given in the case of PP-g-MAH-II in Fig. 9. Although the scatter of the points is significant, the correlation is unambiguous and a reasonable χ_{12} can be determined. The values of χ_{12} are given in Table 3. The χ_{12} parameter is in the order of interaction between non-polar polymers similarly to $\chi_{12}=-0.022$ for iPP/PIB and $\chi_{12}=-0.083$ for iPP/PE blends determined by Pukánszky *et al*. [43, 44]. Ravazi-Nouri *et al*. determined the interaction parameter in iPP/PE blends and the χ_{12} was equal to –0.095 [45]. The interaction parameter is significantly larger in the presence of PP-g-MAH-II, which is an evidence to the fact that χ_{12} depend on further parameters like molecular structure, the length and structure of iPP segments. The calculated interaction parameters indicate the strongest interaction in the presence of PP-g-MAH-II and moderate interaction in the case of PP-g-MAH-I and III. These results are in good agreement with our

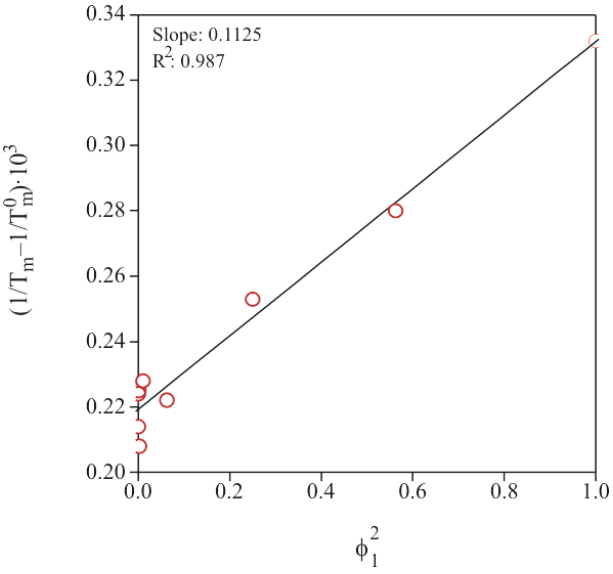

Fig. 9 Plots of the experimental results according to Nishi–Wang theory (Eq. (2) in the case of PP-g-MAH-II

Table 3 The χ_{12} values determined according to Eq. (1)

Blend	χ_{12}
iPP/PP-g-MAH-I	–0.029
iPP/PP-g-MAH-II	–0.119
iPP/PP-g-MAH-III	–0.067

earlier experience, where the most advantageous compatibilizing effect was expressed by PP-g-MAH-II in β-nucleated iPP/PA6 blends [26].

Conclusions

The structure and β-crystallization tendency of PP-g-MAH polymers with different maleic anhydride content were studied. We found that the anhydride content has disadvantageous effect on the crystallization tendency of non-nucleated and β-nucleated PP-g-MAH polymers studied. The higher the anhydride content is, the lower is the crystallization tendency, because the anhydride units disturb the regularity of the iPP chains. Only PP-g-MAH-I with lowest AC crystallises in β-form in the presence of highly active β-nucleating agent. The disadvantageous effect of AC is clearly observable in β-nucleated iPP/PP-g-MAH blends containing 10 mass% of compatibilizer. The presence of PP-g-MAH polymers below 10 mass% does not prevent the formation of β-form in the blends. The peak duplication of the β-phase becomes more pronounced with increasing AC. These results suggest that all of the PP-g-MAH polymers studied can be applied as compatibilizer in β-iPP based blends up to 10 mass% of compatibilizer content.

The interaction between PP-g-MAH polymers and iPP was studied in iPP/PP-g-MAH blends in the whole composition range. The Flory–Huggins interaction parameter (χ_{12}) deduced from calorimetric measurements indicates interaction between the components. The calculated interaction parameters of iPP/PP-g-MAH blends are similar to that of other polyolefin based blends containing non-polar additive polymers. However, we found that the increase of AC in PP-g-MAH polymers is not accompanied by the proportional increase of interaction parameter. The strength of interaction between iPP and PP-g-MAH might depend on further parameters like molecular structure, the length and structure of iPP segments as well. The results indicate clearly that the strength of interaction between iPP and PP-g-MAH compatibilizing agent is one of the key parameter of its compatibilizing effect.

Acknowledgements

The authors would like to express their gratitude to István Sajó for the assistance in wide angle X-ray experiments. Furthermore they should like to acknowledge the Hungarian Research Foundation (OTKA) for supporting the present research (T 49340).

References

1 L. A. Utracki and M. M. Dumoulin, Polypropylene: Structure, Blends and Composites, Vol. 2, J. Karger-Kocsis Ed., Chapmann & Hall, London 1995, p. 50.
2 B. Lotz, J. J. Wittmann and A. J. Lovinger, Polymer, 37 (1996) 4979.
3 J. Varga, J. Macromol. Sci.-Phys., B41 (2002) 1121.
4 C. Grein, Adv. Polym. Sci., 188 (2005) 43.
5 S. C. Tjong, J. S. Shen and R. K. Y. Li, Scr. Metall. Materialia, 33 (1995) 503.
6 J. Karger-Kocsis, J. Varga and G. W. Ehrenstein, J. Appl. Polym. Sci., 64 (1997) 2057.
7 H. B. Chen, J. Karger-Kocsis, J. S. Wu and J. Varga, Polymer, 43 (2002) 6505.
8 J. Varga, J. Thermal. Anal., 35 (1989) 1891.
9 J. Varga and G. Garzó, Angew. Makromol. Chem., 180 (1990) 15.
10 J. Varga, F. Schulek-Tóth and I. Mudra, Macromol. Symp., 78 (1994) 229.
11 C. Grein, C. J. G. Plummer, H. H. Kausch, Y. Germain and P. Beguelin, Polymer, 43 (2002) 3279.
12 A. Menyhárd, J. Varga, A. Liber and G. Belina, Eur. Polym. J., 41 (2005) 669.
13 C. Grein and M. Gahleitner, Express Polym. Lett., 2 (2008) 392.
14 Y. Tao, Y. Pan, Z. Zhang and K. Mai, Eur. Polym. J., 44 (2008) 1165.
15 J. Varga and F. Schulek-Tóth, Angew. Makromol. Chem., 188 (1991) 11.
16 S. C. Tjong, R. K. Y. Li and T. Cheung, Polym. Eng. Sci., 37 (1997) 166.
17 S. C. Tjong and R. K. Y. Li, J. Vinyl Addit. Technol., 3 (1997) 89.
18 F. Ide and A. Hasegawa, J. Appl. Polym. Sci., 18 (1974) 963.
19 S. J. Park, B. K. Kim and H. M. Jeong, Eur. Polym. J., 26 (1990) 131.
20 R. Mülhaupt and J. Rosch, Kunststoffe-Plastics Europe., 84 (1994) 1153.
21 J. Duvall, C. Sellitti, C. Myers, A. Hiltner and E. Baer, J. Appl. Polym. Sci., 52 (1994) 207.
22 A. Gonzalez-Montiel, H. Keskkula and D. R. Paul, J. Polym. Sci. Pt. B-Polym. Phys., 33 (1995) 1751.
23 I. Campoy, J. M. Arribas, M. A. M. Zaporta, C. Marco, M. A. Gomez and J. G. Fatou, Eur. Polym. J., 31 (1995) 475.
24 S. N. Sathe, S. Devi, G. S. S. Rao and K. V. Rao, J. Appl. Polym. Sci., 61 (1996) 97.
25 C. Marco, G. Ellis, M. A. Gomez, J. G. Fatou, J. M. Arribas, I. Campoy and A. Fontecha, J. Appl. Polym. Sci., 65 (1997) 2665.
26 A. Menyhárd and J. Varga, Eur. Polym. J., 42 (2006) 3257.
27 J. Yu and J. S. He, Acta Polym. Sin., (1999) 87.
28 Y. Seo, J. Kim, K. U. Kim and Y. C. Kim, Polymer, 41 (2000) 2639.
29 G. Bogoeva-Gaceva, B. Magnovska and E. Mader, J. Appl. Polym. Sci., 77 (2000) 3107.
30 K. W. Cho, F. K. Li and J. Choi, Polymer, 40 (1999) 1719.
31 C. Vilcu, C. Grigoras and C. Vasile, Macromol. Mater. Eng., 292 (2007) 445.
32 J. Varga and G. W. Ehrenstein, Polymer, 37 (1996) 5959.
33 J. Varga, I. Mudra and G. W. Ehrenstein, J. Appl. Polym. Sci., 74 (1999) 2357.

34 R. H. Olley and D. C. Bassett, Polymer, 23 (1982) 1707.
35 A. Turner-Jones, J. Aizlewood, M. and D. Beckett, Macromol. Chem., 75 (1964) 134.
36 A. Menyhárd, J. Varga and G. Molnár, J. Therm. Anal. Cal., 83 (2006) 625.
37 J. Varga, Polypropylene: Structure, Blends and Composites, Vol. 1, J. Karger-Kocsis Ed., Chapmann & Hall, London 1995, p. 56.
38 J. Varga and G. W. Ehrenstein, Colloid Polym. Sci., 275 (1997) 511.
39 T. Nishi and T. T. Wang, Macromolecules, 8 (1975) 909.
40 B. Monasse and J. M. Haudin, Colloid Polym. Sci., 266 (1988) 679.
41 B. Monasse and J. M. Haudin, Colloid Polym. Sci., 263 (1985) 822.
42 P. Szabó and B. Pukánszky, Macromol. Symp., 129 (1998) 29.
43 P. Szabó, E. Epacher, K. Belina and B. Pukánszky, Macromol. Symp., 129 (1998) 137.
44 P. Szabó, E. Epacher, E. Földes and B. Pukánszky, Mater. Sci. Eng. A., 383 (2004) 307.
45 M. Razavi-Nouri, Polym. Test, 26 (2007) 108.

Received: November 15, 2007
Accepted: June 24, 2008

DOI: 10.1007/s10973-007-8569-7